Control Engineering Practice 13(6):739–748, 2005

Genetic Algorithms Optimisation of Decoupled Sliding Mode Controllers: Simulated and Real Results

E. Alfaro-Cid[a], E.W. McGookin[a], D.J. Murray-Smith[a], T.I. Fossen[b]

[a] Department of Electronics and Electrical Engineering, University of Glasgow, Rankine Building, Oakfield Av., G12 8LT Glasgow, UK

[b] Department of Engineering Cybernetics, Norwegian University of Science and Technology, N-7491 Trondheim, Norway

Abstract

Two decoupled Sliding Mode control configurations have been designed for the navigation and propulsion systems of *CyberShip II*, a scale model of an oil platform supply ship. These control structures have parameters that need to be tuned to improve their performance. These parameters have been optimised using Genetic Algorithms. The performance of these controllers has been analysed through computer-generated simulations based on a non-linear hydrodynamic model of *CyberShip II*. The robustness has been evaluated through simulation in the presence of environmental disturbances. Subsequently, the optimised controllers have been tested in the real plant and the results are shown.

1. Introduction

Navigation of ships has been a major concern for sailors and stakeholders since humans took to the waters. Approaches involving nautical sextants and the judgement of the navigator, have been superceded by the introduction of advanced technology that assists with the sailing process. However, the size, number and versatility of modern ships has highlighted the need for better navigational control in order to avoid accidents.

In order to ensure the safe navigation of surface vessels, their motion (i.e. navigation and propulsion capabilities) has to be controlledaccurately. This can be achieved through the design and implementation of automatic control systems that can accurately govern the manoeuvring capabilities of ships.

There are many control methodologies that have their own structure and can be used for this purpose (Dutton, Thompson, & Barraclough, 1997; Slotine & Li, 1991). The performance of these controllers depends not only on the control structure but also on the values of the controller's parameters. Conventionally, these parameters are manually tuned by the designer, who attempts to find an acceptable controller solution. However, this relies on an ad hoc approach to tuning, which depends on the experience of the designer. If the designer is not experienced, this process can become tedious and time consuming. In either case, there is no guarantee that the designed solution will perform satisfactorily as the tuning process depends on the qualitative judgement of the designer.

A solution to this problem is to use optimisation techniques that tune such parameters automatically. The most powerful of these techniques is based on Genetic Algorithms (GAs) (Holland, 1992; Goldberg, 1989). GAs are optimisation techniques that mimic the way species evolve in nature. They operate on a population of potential solutions to a given problem by applying the

Darwinian principal of "survival of the fittest". At each generation, a new set of candidate solutions is created by the process of selecting individuals according to their level of fitness (the better the performance of the solution, the fitter it is) and breeding them together using operators borrowed from natural genetics. This process leads to the evolution of populations of better possible solutions to a given problem.

This paper covers the optimisation of control systems for the propulsion and navigation of an oil platform supply ship using a GA. The particular vessel used in this study is a scale model called *CyberShip II* (CS2) (Lindegaard & Fossen, 2002) which is the test vehicle for the Marine Cybernetics Laboratory (MCLab) at the Norwegian University of Science and Technology (NTNU). Computer-generated simulations based on a nonlinear hydrodynamic model of CS2 are used in the optimisation studies.

The particular control methodology considered in this work is a decoupled nonlinear Sliding Mode (SM) control (Healey & Marco, 1992; Healey & Lienard, 1993; Slotine & Li, 1991; Utkin, 1972). Two SM controllers are used to provide the structure for propulsion control (for governing surge velocity) and navigation control (for governing heading). The goal of this study is to obtain controller solutions that satisfactorily perform these duties while keeping actuator usage to a minimum. The GA solves this minimisation problem by evolving controller solutions that satisfy these objectives.

Also, GA optimisations in the presence of simulated environmental disturbances (wind-generated waves) (Fossen, 1994) are carried out. The objective is to see if by including a realistic noisy environment in the simulation, the GA can improve the robustness of the controller.

Subsequently, all the optimised controllers have been implemented in the real plant and tested in the water basin of the MCLab at NTNU. Similar trials manoeuvres to those in the simulations were used in that part of the study.

The results obtained from this study illustrate the benefits of using GAs to optimise propulsion and navigation controllers for surface ships.

2. CyberShip II

2.1. Marine cybernetics lab

The model subject used in this work is CS2. CS2 is a scale model (scale $\frac{1}{70}$th approx.) of an oil platform supply ship, which has been developed at the Department of Engineering Cybernetics at NTNU. The testing of the optimised controllers in the real model has been performed in the MCLab at NTNU. The MCLab is an experimental laboratory for testing of ships and underwater vehicles.

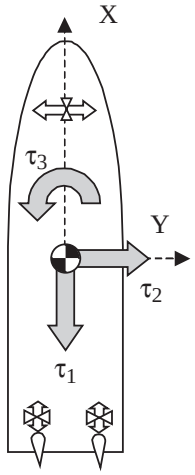

Fig. 1. Actuator's position in CS2.

The length of CS2 is 1.255 m and its mass is 23.8 kg. It is actuated by means of a tunnel-thruster placed at the bow and two main propellers with rudders situated at the stern as shown in Fig. 1.

For position measurement purposes, CS2 is fitted with three three-dimensional emitters. The signals emitted are detected by four PC/cameras that provide the measurements of the (x, y) coordinates plus the heading angle to the user.

CS2 is also equipped with an onboard PC running QNX real-time operating system. The control calculations are performed in real-time by an onshore PC. The connection between both PCs is made through a wireless Ethernet link and an automatic C-code generator. Matlab Simulink and Real Time Workshop are coupled with a graphical user interface in LabView to provide a real-time presentation of the results.

The MCLab is also equipped with a wave generator. Such a generator consists of a single flap controlled by a wave synthesiser that can produce regular and irregular waves with various spectra and wave height. The wave generator is used in the experimental trials in this study.

For more accurate information about the MCLab and CS2 refer to Lindegaard and Fossen (2002), Corneliussen (2003) and Sveen (2003).

2.2. Mathematical model of CyberShip II

Prior to the real testing in the MCLab, the optimisation and design of the controllers for CS2 have been conducted using a non-linear hydrodynamic model based on the kinetic and kinematic equations that represents the dynamics of the vessel (Fossen, 1994). When these kinetic and kinematic equations are combined together the following matrix form is

produced (assuming $\mathbf{M}$ to be invertible):

$$\begin{bmatrix} \dot{\mathbf{v}} \\ \dot{\boldsymbol{\eta}} \end{bmatrix} = \begin{bmatrix} -\mathbf{M}^{-1}(\mathbf{C}(\mathbf{v}) + \mathbf{D}) & \mathbf{0} \\ \mathbf{J}(\boldsymbol{\eta}) & \mathbf{0} \end{bmatrix} \cdot \begin{bmatrix} \mathbf{v} \\ \boldsymbol{\eta} \end{bmatrix} + \begin{bmatrix} \mathbf{M}^{-1} \\ \mathbf{0} \end{bmatrix} \cdot \boldsymbol{\tau}. \tag{1}$$

Here $\mathbf{M}$ is the mass/inertia matrix, $\mathbf{C}$ is the Coriolis matrix, $\mathbf{D}$ is the damping matrix and $\mathbf{J}$ is the Euler matrix. Also, $\mathbf{v} = [u, v, r]^{\mathrm{T}}$ is the body-fixed linear and angular velocity vector, $\boldsymbol{\eta} = [x, y, \psi]^{\mathrm{T}}$ denotes the position and orientation vector with coordinates in the earth-fixed frame and $\boldsymbol{\tau} = [\tau_1, \tau_2, \tau_3]^{\mathrm{T}}$ is the input force vector, given that τ_1, τ_2 and τ_3 are the forces along the body-fixed X- and Y-axes, and the torque about the body-fixed Z-axis, respectively (see Fig. 1).

This expression corresponds to a non-linear state-space equation in the form:

$$\dot{\mathbf{x}} = \mathbf{A}(\mathbf{x}) \cdot \mathbf{x} + \mathbf{B} \cdot \boldsymbol{\tau}. \tag{2}$$

2.3. Environmental disturbances

In order to evaluate the robustness against environmental disturbances of the controllers obtained through the GA optimisation, simulations of manoeuvres in the presence of environmental disturbances have been carried out.

There are three main types of environmental disturbances: wind-generated waves, ocean currents and wind. However, in this research the analysis has been restricted to the disturbance considered to be the most relevant for surface vessels, i.e. wind-generated waves. In addition they are the only environmental disturbance that can be reproduced in the MCLab for testing.

The model that has been used to simulate the wave's action on the vessel derives the forces and moments induced by a regular sea on a block-shaped ship and it is described in Zuidweg (1970). It forms a vector called $\boldsymbol{\tau}_{waves}$ that is directly added to the input vector, $\boldsymbol{\tau}$, in Eq. (1) using the principle of superposition.

$$\begin{aligned} X_{wave}(t) &= \sum_{i=1}^{N} \rho g B L T \cos(\beta - \psi) s_i(t), \\ Y_{wave}(t) &= \sum_{i=1}^{N} -\rho g B L T \sin(\beta - \psi) s_i(t), \\ N_{wave}(t) &= \sum_{i=1}^{N} \frac{1}{24} \rho g B L (L^2 - B^2) \sin 2(\beta - \psi) s_i^2(t). \end{aligned} \tag{3}$$

Here L, B and T are the length, breadth and draft of the wetted part of a ship, considering it as a parallelepiped. ρ is the density of the water, $s_i(t)$ the wave slope, and $(\beta - \psi)$ the angle between the heading of the ship and the direction of the wave (in radians).

The wave slope, s_i can be related to the wave spectral density function $S(\omega_i)$. To compute $S(\omega_i)$ different wave spectra can be considered. In this study a modified version of the Pierson–Moskowitz spectrum has been used Fossen (1994)

$$S(\omega) = \frac{4\pi^3 H_s^2}{(0.710 T_o)^4 \omega^5} \exp\left(\frac{-16\pi^3}{(0.710 T_o)^4 \omega^4}\right). \tag{4}$$

Here, T_o is the modal period and H_s, the significant wave height.

3. Sliding Mode (SM)

3.1. Theoretical background

SM control (Slotine & Li, 1991; Utkin, 1972) is considered to be a robust control methodology and therefore able to handle changes in the plant and external disturbances without assignificant performance degradation. The structure of a SM controller is composed of a nominal part plus an additional term aimed at providing additional control effort for dealing with disturbances.

The control problem to be solved with an SM controller is to make the system response track a specified desired trajectory. This is achieved by comparing the actual states to be controlled ($\mathbf{x}$) with the desired states ($\mathbf{x}_d$). SM control constructs a surface that is a function of the tracking error, $\tilde{\mathbf{x}} = \mathbf{x} - \mathbf{x}_d$, called the *sliding surface* ($\sigma(\tilde{\mathbf{x}})$) (Edwards & Spurgeon, 1998; Healey & Lienard, 1993; Healey & Marco, 1992; Slotine & Li, 1991; Utkin, 1972). Then, the n-dimensional problem of solving $\tilde{\mathbf{x}} = 0$ is reduced to driving the sliding surface to zero. The SM controller provides a control input that drives the system to the sliding surface. Once the system is on the sliding surface is said to be in the *sliding mode* (Edwards & Spurgeon, 1998; Slotine & Li, 1991; Utkin, 1972). Therefore, the problem of tracking $\mathbf{x}_d$ is equivalent to that of remaining on the zero sliding surface for all $t > 0$ (McGookin, 1997; Slotine & Li, 1991).

For SM control the plant input has two distinct components (Edwards & Spurgeon, 1998; McGookin, 1997; Slotine & Li, 1991): the equivalent control (u_{eq}) and the switching term (u_{sw}). The equivalent control provides the main control action, while the switching signal ensures the discontinuity of the control law across ($\sigma(\tilde{\mathbf{x}})$), supplying additional control to account for the presence of matched disturbances and unmodeled dynamics.

The equivalent component of the control action is usually chosen as a linear controller. In this case a feedback gain controller of the following form (Fossen,

1994; McGookin, 1997; Mudge & Patton, 1988) is used:

$$u_{eq} = -\mathbf{k}^{\mathrm{T}} \cdot \mathbf{x}, \tag{5}$$

where $\mathbf{k}$ is a feedback gain obtained from robust Pole Placement theory according to the method proposed by Kaustky, Nichols, and Van Dooren (1985). This method is chosen since it minimises the sensitivity of the closed-loop poles to perturbations in the coefficients of the matrices of the system.

The switching term is a non-linear term that provides the additional control action to counteract disturbances in the plant. This switching control action is designed round the sliding surface $\sigma(\hat{\mathbf{x}})$. The sliding surface has to be chosen so that as the surface value tends to zero the state error tends to zero as well.

The sliding surface used in this work is as follows (Healey & Lienard, 1993; Healey & Marco, 1992; McGookin, 1997):

$$\sigma(\hat{\mathbf{x}}) = \mathbf{h}^{\mathrm{T}} \cdot \hat{\mathbf{x}}, \tag{6}$$

where $\mathbf{h}$ is the right eigenvector of the desired closed-loop system matrix $\mathbf{A}_c$ and $\hat{\mathbf{x}} = \mathbf{x} - \mathbf{x}_d$ is the state error vector. The switching term can be obtained by taking the derivative of Eq. (6). A complete derivation of this term can be found in McGookin (1997) and yields

$$u_{sw} = \left(\mathbf{h}^{\mathrm{T}}\mathbf{b}\right)^{-1}\left(\mathbf{h}^{\mathrm{T}}\dot{\mathbf{x}}_d - \eta \cdot \mathrm{sgn}(\sigma(\hat{\mathbf{x}}))\right). \tag{7}$$

where η is the called switching gain, which determines the magnitude of the additional switching action of the controller. Hence, the resulting controller

$$u = -\mathbf{k}^{\mathrm{T}} \cdot \mathbf{x} + (\mathbf{h}^{\mathrm{T}}\mathbf{b})^{-1}(\mathbf{h}^{\mathrm{T}}\dot{\mathbf{x}}_d - \eta \cdot \mathrm{sgn}(\sigma(\hat{\mathbf{x}}))). \tag{8}$$

The additional control effort provided by the switching term, while beneficial to improve robustness, can also lead to a phenomenon called *chattering* (Edwards & Spurgeon, 1998; McGookin, 1997). The chattering is due to the inclusion of the sign function in the switching term and it can cause the control input to start oscillating around the zero sliding surface, resulting in unwanted wear and tear of the actuators.

One way to solve the problem is to smooth the switching term as the sliding surface gets closer to zero (*soft switching*). In this study, this has been achieved by using the continuous hyperbolic tangent function instead of the discontinuous sign function. The hyperbolic tangent function has the same asymptotes as the sign function, but around the zero σ value there is a gradual transition area (called the *boundary layer*). The width of this boundary layer is defined by the *boundary layer thickness* (Φ) (McGookin, 1997).

The boundary layer thickness has to be large enough to counteract the large switching action. However, if it is too large, the switching action will be replaced by proportional control action.

Hence, the final controller equation becomes

$$u = -\mathbf{k}^{\mathrm{T}} \cdot \mathbf{x} + (\mathbf{h}^{\mathrm{T}}\mathbf{b})^{-1}\left(\mathbf{h}^{\mathrm{T}}\dot{\mathbf{x}}_d - \eta \tanh\left(\frac{\sigma(\hat{\mathbf{x}})}{\phi}\right)\right). \tag{9}$$

Here, the boundary layer transition is applied through a continuous tanh function.

3.2. Controller implementation

As already mentioned, the system has been decoupled for the SM control. As shown in Eqs. (10) and (11), the heading subsystem consists of three states ($\mathbf{x}_H = [v, \psi, r]$), and one input ($u_H = \tau_3$). Meanwhile, the propulsion subsystem consists of a single state ($x_P = u$), and one input ($u_P = \tau_1$)

$$\dot{u} = \mathrm{a}_p \cdot u + \mathrm{b}_p \cdot \tau_1, \tag{10}$$

$$\begin{bmatrix} \dot{v} \\ \dot{r} \\ \dot{\psi} \end{bmatrix} = \mathbf{A}_h(v, r, \psi) \cdot \begin{bmatrix} v \\ r \\ \psi \end{bmatrix} + b_h \cdot \tau_3. \tag{11}$$

Then, the control actions become (Alfaro-Cid, McGookin, & Murray-Smith, 2001a; McGookin, 1997)

$$\tau_1 = -\mathbf{k}_p^{\mathrm{T}}u + (\mathbf{h}_p^{\mathrm{T}}\mathbf{b}_p)^{-1}\left(\mathbf{h}_p^{\mathrm{T}}\dot{u}_d - \eta_p \tanh\left(\frac{\sigma_p(u - u_d)}{\phi_p}\right)\right), \tag{12}$$

$$\tau_3 = -\mathbf{k}_h^{\mathrm{T}}\mathbf{x}_h + (\mathbf{h}_h^{\mathrm{T}}\mathbf{b}_h)^{-1}\left(\mathbf{h}_h^{\mathrm{T}}\dot{\mathbf{x}}_{hd} - \eta_h \tanh\left(\frac{\sigma_h(\mathbf{x}_h - \mathbf{x}_{hd})}{\phi_h}\right)\right). \tag{13}$$

In order to achieve the desired control action, there are four key parameters to optimise for the heading SM controller: two poles in the equivalent term and η_h and Φ_h in the switching term. In the same way, there are three parameters to optimise for the propulsion control: one pole in the equivalent term, η_p and Φ_p in the switching term.

4. Genetic algorithms

GAs (Goldberg, 1989; Holland, 1992) are optimisation techniques that mimic the way species evolve in nature. Two mechanisms are the key element in the evolution of many species: the Darwinian natural selection and sexual reproduction. The genetic operators involved in sexual mating allow the offspring to inherit the features from both its parents. GAs emulate this process by evolving a population of parameter solutions to a given problem through a predetermined number of generations.

Parameter Encoding = abcde

Parameter Value = $(a+0.1b+0.01c+0.001d)\times 10^{(e/2-2)}$

Fig. 2. Parameter encoding.

4.1. Encoding

The elements of the space of possible solutions or *search space* must be suitably encoded as a string of integers so that the GA can work with them. These integers are called genes. Each weighting parameter value is encoded as a string of five genes (McGookin, 1997). Since there are seven parameters to optimise each possible solution is represented by a *chromosome* that is a string of 35 genes. These genes, instead of being binary bits (as they used to be in the traditional GA), are integers included within the interval (0, 9), in order to allow a wide range of possible values (from 0.001×10^{-2} to 9.999×10^{3}) in smaller chromosomes (Fig. 2).

4.2. Cost function

Once an initial population of chromosomes is generated at random, the chromosomes are decoded to obtain the corresponding controller's parameter values and these are implemented in the controllers. The controller's performance is evaluated through simulation of the system being controlled.

The optimisation design criteria are defined by the cost function in Eq. (14). In addition to this there is a desired response that the controller must track. The desired heading and propulsion manoeuvres used in the GA optimisation are two critically damped steps of 45° and 0.2 m/s, respectively.

The cost function will have three terms for each controller (Alfaro-Cid et al., 2001a, b). It is a single objective, multi-aspect criterion

$$C = \sum_{i=0}^{tot}\left[(\Delta\psi_i)^2 + \lambda_1(\tau_{3i})^2 + \mu_1\left(\frac{\tau_{3i}-\tau_{3i-1}}{\Delta t}\right)^2\right] + \sum_{i=0}^{tot}\left[(\Delta u_i)^2 + \lambda_2(\tau_{1i})^2 + \mu_2\left(\frac{\tau_{1i}-\tau_{1i-1}}{\Delta t}\right)^2\right], \quad (14)$$

where *tot* is the total number of iterations, $\Delta\psi_i$ is the *i*th heading angle error between the desired and resulting heading, τ_{3i} is the *i*th yaw thrust force, Δu_i is the *i*th surge velocity error between the desired and resulting surge velocity and τ_{1i} is the *i*th surge thrust force.

The third and sixth terms introduce a measurement of the inputs increasing or decreasing rates (Alfaro-Cid et al., 2001a, b). These terms reduce the oscillations in the inputs, avoiding any unnecessary wearing and tearing of the actuators that shortens their lifespan.

As the input force and torque are always larger than the output errors near the optimum, they dominate the cost values in this crucial area. This imbalance leads to solutions that provide very small thruster effort but, a very poor tracking of the desired responses. In order to avoid this four scaling factors are introduced, so that an equally balanced trade-off between the elements is obtained and all the terms of the cost function are equally optimised.

4.3. GA basic operators

There are three main operators that constitute the GA search mechanism: *selection, crossover* and *mutation*.

The selection procedure depends on the quantified evaluation of each candidate solution that is obtained from the cost function. Selection determines which solutions are chosen for mating according to the principal of survival of the fittest (i.e. the better the performance of the solution, the more likely it is to be chosen for mating and the more offspring it produces).

Once the new population has been selected, chromosomes are ready for crossover and mutation.

The crossover operator combines the features of two parents to create new solutions. Crossover allows an improvement in the species in terms of the evolution of new solutions that are fitter than any seen before. One or several crossover points are selected at random on each parent and then, complementary fractions from the two parents are spliced together to form a new chromosome.

The mutation operator alters a copy of a chromosome reintroducing values that might have been lost or creating totally new features. One or more locations are selected on the chromosome and replaced with new randomly generated values.

The three operators are implemented iteratively. Each iteration produces a new population of solutions, which is called a *generation*. The GA continues to apply the operators and evolve generations of solutions until a near optimum solution is found or a finite number of generations is produced.

5. Optimisation procedure

In this study, a GA is used to optimise the parameters of the decoupled SM controllers. The GA model used has been: tournament selection (with tournament size equal to 8); exponential and non-uniform mutation and double point crossover with a probability of 0.8. This choice is supported by the results obtained in a comparison study of various GA schemes (Alfaro-Cid, 2003). The population size has been 80 and the number of generations 50. This GA configuration has been run 15 times in order to analyse the performance of the method and any similarity in the solutions that have been obtained.

The parameters to optimise for minimising the cost function from Eq. (14) are two poles ($pole_{h1}$ and $pole_{h2}$), the switching gain (η_h) and the boundary layer thickness (Φ_h) for heading. For propulsion, one pole ($pole_{p1}$), the switching gain (η_p) and the boundary layer thickness (Φ_p) for the SM configuration outline in Section 3.

The pair of poles of the equivalent term for the heading subsystem can be either real poles or a complex conjugate pair. Only the magnitude of the poles has been optimised, the sign is added in the decoding operator to ensure that they are in the left-hand side of the s-plane. The switching gain and boundary layer thickness have to be positive to ensure stability robustness (McGookin, 1997).

The inclusion of waves in the simulations improves the realism of the evaluation and allows the potential of the GA to produce more robust controllers to be analysed. As a result the SM controllers have been optimised in two different ways: with and without the inclusion of waves in the simulation.

The final evaluation stage involves testing the optimised results in the water basin of the MCLab in NTNU. The path tracking manoeuvre used for the trials is again a zig-zag manoeuvre. These physical trials are performed in the presence of waves.

6. Results

6.1. Description of the experiments

The final evaluation stage involves testing the optimised results in the water basin of the MCLab in NTNU. These physical trials are performed in the presence of waves.

The optimised controller results have been tested executing a path tracking zig-zag manoeuvre. This manoeuvre has been chosen to reproduce the 45° turning manoeuvre used in the simulation work. The zig-zag is tracked at a constant surge speed of 0.2 m/s, approximately.

Also, the manoeuvre is executed while generating waves in order to study their effect. The waves synthesizer is set to generate irregular waves with a Pierson–Moscowicz spectrum (Fossen, 1994), like the one used in simulations. The significant wave height is 5 mm (scale 1/70th) and the peak period of 0.80 s. The initial angle of attack of the waves is 0°. This is defined by the fixed position of the flap that generates the waves in the tank. This angle changes along the manoeuvre due to the turning of the boat.

Regarding the actuators of the boat, once the controller produces the commanded forces vector, based on the state errors, these forces and moment have to be allocated to the actuators. This is achieved by implementing an algorithm that calculates the values for propeller speed and rudder deflection in an optimal manner (Lindegaard & Fossen, 2002). The algorithm optimises the fuel efficiency of the actuators while eliminating discontinuities in the signals that would produce excessive wearing in the thrusters.

6.2. Optimisation without waves: simulated and real results

The best result is obtained when the GA search converges to a cost value of 4.5, with the parameters from Table 1. The GA has converged to the near-optimal solution in 14 generations.

When averaging the gain results obtained through different runs, the average and standard deviation values are shown in Table 2.

Although the poles converge to very similar values (small standard deviations), that is not the case of the switching gain η and boundary layer width Φ. However, if instead of comparing the values of η and Φ, we take into account the ratio between them, there is a clear convergence. This can be due to the SM controller operating not in the switching range of the hyperbolic tangent function but in the boundary layer McGookin (1997). If so, the controller acts as a proportional control action and the ratio η/Φ drives the performance of the controller, not the individual values for η and Φ.

Fig. 3 shows the simulated performance of the SM controllers when tracking the zig-zag manoeuvre used in the GA optimisation.

The heading results present a slight overshooting in the heading response, due to SM being a high gain controller. The propulsion tracking is very good, keeping the surge error always under 4 mm/s, although it shows a small steady state error. The actuator's signals are free from rippling. The heading control shows two spikes that correspond with the beginning of the turn. They are due to the high gain of the system that reacts very quickly to the change and then it needs to overcompensate.

The results obtained while implementing the optimised controllers in the real plant are plotted in the next graphs. In Fig. 4, the testing manoeuvre is performed without waves. CS2 tracks a zig-zag manouvre for heading as in the simulation test. However, the zig-zag reference signal for the surge speed could not be reproduced in the real testing due to the lack of

Table 1
Best results—optimisation without waves

	p_1	p_2	η	Φ
Propulsion	−0.01	N/A	0.791	0.17
Heading	−1.4	−0.25	3.8	1.991

Table 2
Average and standard deviation results—optimisation without waves

	$Pole_1$		$Pole_2$		η		Φ		η/Φ	
	Avg	Std. Dev.	Avg	Std. Dev.	Avg	Std. Dev.	Avg	Std. Dev.	Avg	Std. Dev.
Prop.	−0.013	0.005	N/A	N/A	1508	2676	310.6	565.8	5.17	0.71
Heading	−1.078	0.352	−0.286	0.036	415.4	574.1	201.1	277.1	2.07	0.23

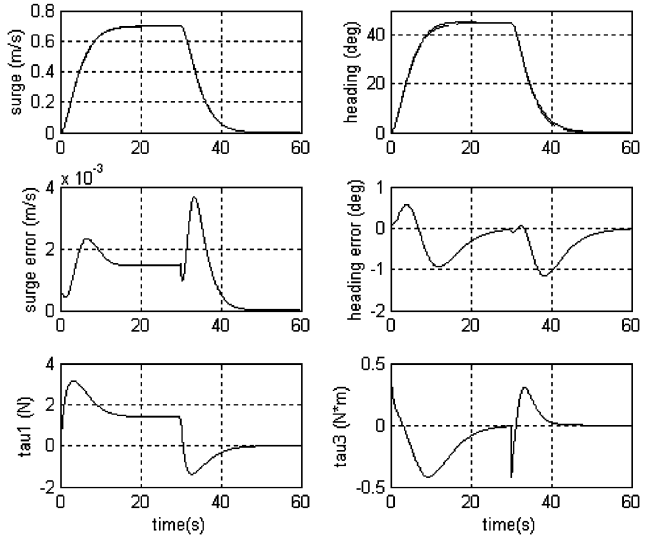

Fig. 3. Simulated results of the SM controller optimised without waves.

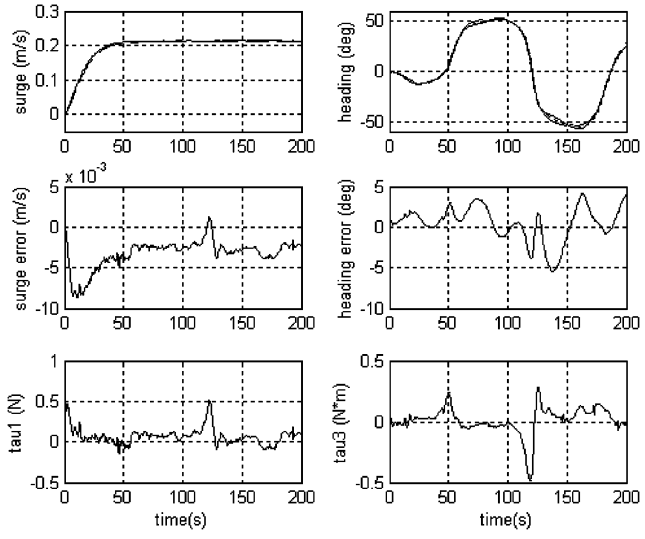

Fig. 4. Real results of the SM controller optimised without waves when manoeuvring in calm waters.

accuracy of the apparatus used to regulate the propulsion.

Again the tracking is good, although the heading tracking degrades a bit in the second half of the zig-zag.

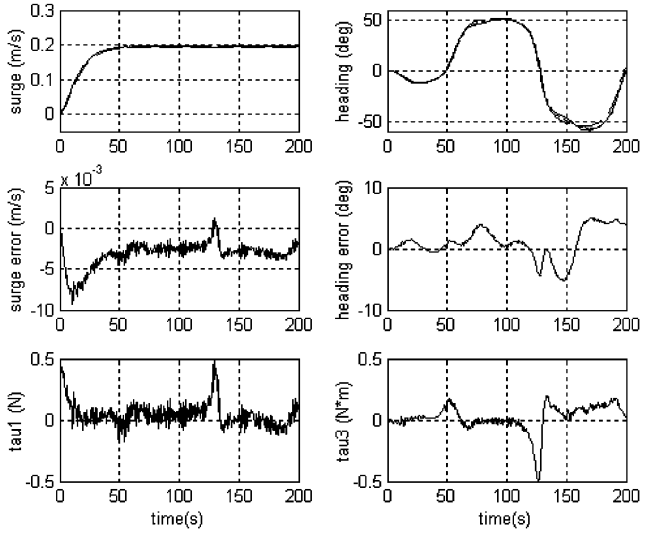

Fig. 5. Real results of the SM controller optimised without waves when manoeuvring in calm waters.

This is probably due to the increased difficulty of a second turning just when the boat was recovering from the first. The heading error is small and, although there are some peaks in the control signal the control effort for SM is small. Regarding the propulsion subsystem, the results are very satisfactory. Fig. 5 shows the results obtained by CS2 when performing the same manoeuvre but in the presence of waves in the water tank.

It can be observed from the figure that the inclusion of waves does not degrade the tracking significantly. However, it induces high-frequency components in the signals, especially in the propulsion subsystem. This is caused by the high-gain nature of this methodology, which will make the input signals follow the disturbance in order to compensate for their effect.

6.3. Optimisation with waves: simulated and real results

For the optimisation with waves, the GA has converged in nine generations. The best result has a cost value of 11.5, with the following parameters values as given in Table 3.

When averaging the gain results obtained through 15 runs, the average and standard deviation values are given in Table 4.

When comparing these optimised results with those of Tables 1 and 2 it can be observed that including waves in the simulation makes the GA converge to a similar heading controller with somewhat closer poles and analogous η/Φ ratio. Closer poles lead to a more underdamped response.

On the other hand, the GA search converges to a quite different propulsion controller where the pole is closer to zero and the η/Φ ratio has been reduced by one order of magnitude. By placing the propulsion pole closer to zero the GA is trying to achieve an integral action that will improve the tracking. Moreover, reducing the ratio η/Φ will reduce the gain of the controller, given that SM is operating in the boundary layer.

Fig. 6 shows the simulated performance of the decoupled SM controllers when tracking the zig-zag manoeuvre for surge and heading used in the GA optimisation with waves. The desired responses have been represented by a dashed line.

The above figure shows very good surge tracking during the first half of the zig-zag (when the encounter angle between the heading and the direction of the waves is 90°). However, the tracking is worse the initial stages of the first transient and in the second half of the manoeuvre (when the encounter angle between the heading and the direction of the waves is 135°). It seems that the SM propulsion controller handles lateral waves better than approaching ones. The degradation of the performance at the end of the surge response is due to the slow surge speed that diminishes the effectiveness of the actuators for compensating the waves effect. Consequently, the slow speed and relative position of the vessel to the waves makes the propulsion system particularly susceptible to the noise induced errors caused by the wave motion.

Next Figs. 7 and 8 illustrate the results obtained in the real tests in the MCLab when the SM controllers had been implemented in the real plant. Fig. 7 shows the execution of the manoeuvre in calm waters.

The set of plots shows that this tuning solution for the SM controller provides very good heading tracking, but quite poor propulsion control. There is a large steady-

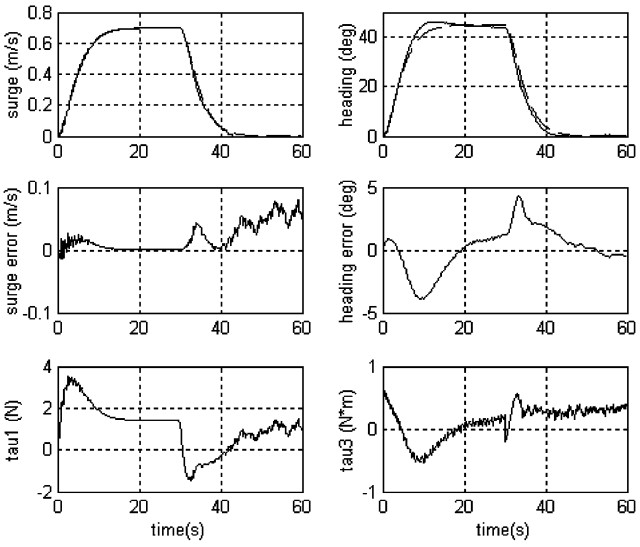

Fig. 6. Simulated results of the SM controller optimised with waves.

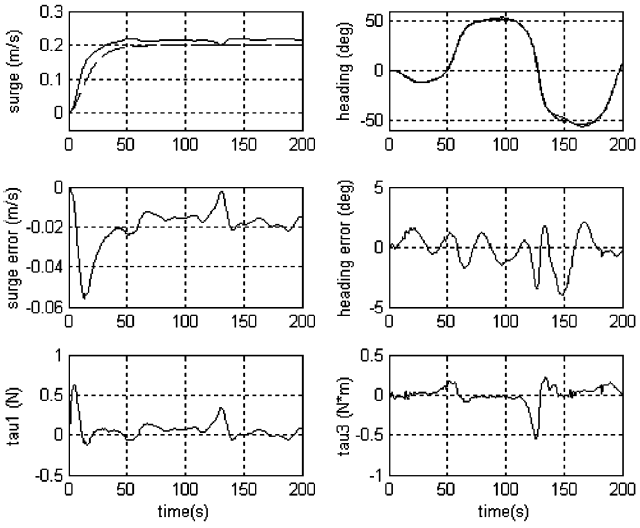

Fig. 7. Real results of the SM controller optimised with waves when manoeuvring in calm waters.

Table 3
Best results–optimisation with waves

	p_1	p_2	η	Φ
Prop.	−0.001		762.5	864
Heading	−0.945	−0.432	9.05	4.305

Table 4
Average and standard deviation results—optimisation with waves

	Pole_1		Pole_2		η		Φ		η/Φ	
	Avg	Std. Dev.	Avg	Std. Dev.	Avg	Std. Dev.	Avg	Std. Dev.	Avg	Std. Dev.
Prop.	−0.003	0.0028			1822	2386	2384	3271	0.79	0.09
Heading	−0.974	0.2939	−0.466	0.0620	1484	3114	880	1944	1.85	0.29

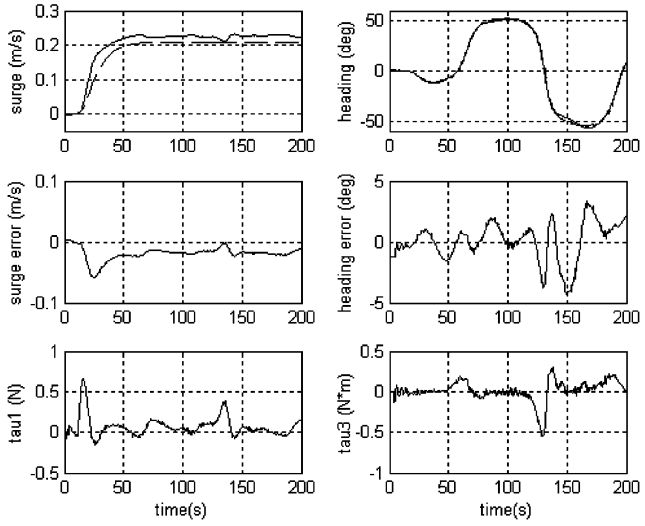

Fig. 8. Real results of the SM controller optimised with waves when manoeuvring in the presence of waves.

state error in surge speed and the signal is quite oscillatory.

Fig. 8 illustrates the results obtained when the zig-zag manoeuvre is performed in the presence of waves.

When including waves, they do not affect the heading and propulsion tracking and the commanded force signals are definitely less influenced than those of the SM controller optimised without disturbances.

The controller optimised with waves provides smoother commanded signals than the one optimised without waves, while the propulsion tracking degrades when optimised in the presence of waves.

7. Conclusions

The results obtained in the GA optimisation without waves are very good. The tracking is satisfactory and the controller signals are smooth.

When the controllers obtained in the GA optimisation without waves are tested in the presence of waves the tracking performance does not degrade significantly. The main effect of the waves is the noise induced in the commanded forces (especially τ_1). This allows the controllers to be assessed for their disturbance rejection performance.

Regarding the optimisation carried out with simulated waves, the objective was to ensure that the GA gives a more robust controller (i.e. an improved performance in the presence of environmental disturbances). However, if we compare the performance of the controllers optimised with, and without waves, it can be observed that those controllers optimised with waves do not provide a better performance. The GA concentrates on reducing the ripple in τ_1 (the main effect of the waves) by reducing the control action in order to improve the cost function value and that degrades the performance of the propulsion controllers. Therefore the propulsion controllers optimised with waves are characterised by a reduction in control effort and a very poor propulsion response. On the other hand, the navigation subsystem is less sensitive to the effect of waves. Consequently, the resulting heading controller parameters in the optimisation with waves are similar to those obtained in the GA optimisation without waves. This can be due to the sluggish propulsion dynamics. The controller tries to react to the noise but due to the slow actuator dynamics, overcompensates and ends up producing oscillatory responses.

As a result, the advantage of including noise in the simulation lies in obtaining controller solutions with smoother control signals that are able to reduce wear and tear of actuators. However, including waves in the optimisation scenario does not improve the performance robustness and disturbance rejection abilities of the controller solutions.

References

Alfaro-Cid, E. (2003). *Optimisation of time domain controllers for supply ships using genetic algorithms and genetic programming*. Ph.D. thesis, University of Glasgow, UK.

Alfaro-Cid, E., McGookin, E. W., & Murray-Smith, D. J. (2001a). Genetic algorithm optimisation of a supply ship propulsion and navigation systems, *Proceedings of the MTS/IEEE oceans conference*, Honolulu, USA (pp. 2645–2652).

Alfaro-Cid, E., McGookin, E. W., & Murray-Smith, D. J. (2001b). Genetic algorithm optimisation of a ship navigation system. *Acta Polytechnica*, *41*(4–5), 13–19.

Corneliussen, J. (2003). *Implementation of a guidance system for CyberShip II*. Master thesis, Norwegian University of Science and Technology, Trondheim, Norway.

Dutton, K., Thompson, S., & Barraclough, B. (1997). *The art of control engineering*, Harlow: Addison-Wesley.

Edwards, C., & Spurgeon, S. K. (1998). *Sliding mode control: theory and applications*, London: Taylor & Francis Ltd.

Fossen, T. I. (1994). *Guidance and control of ocean vehicles*, Chichester: Wiley.

Goldberg, D. (1989). *Genetic algorithms in searching optimisation and machine learning*, Reading, MA: Addison-Wesley.

Healey, A. J., & Lienard, D. (1993). Multivariable sliding mode control for autonomous diving and steering of unmanned underwater vehicles. *IEEE Journal of Oceanic Engineering*, *18*(3), 327–339.

Healey, A. J., & Marco, D. B. (1992). Slow speed flight control of autonomous underwater vehicles: experimental results with NPS AUV II. *Proceedings of the second international offshore and polar engineering conference,* San Francisco (pp. 523–532).

Holland, J. H. (1992). *Adaptation in natural and artificial systems*, Cambridge, MA: MIT Press.

Kaustky, J., Nichols, N. K., & Van Dooren, P. (1985). Robust pole assignment in linear state feedback. *International Journal of Control*, *41*, 1129–1155.

Lindegaard, K. P., & Fossen, T. I. (2002). Fuel efficient rudder and propeller control allocation for marine craft: experiments with a

model ship. *IEEE Transactions on Control Systems Technology*, *TCST-11*(6), 850–862.

McGookin, E. W. (1997). *Optimization of sliding mode controllers for marine applications: a study of methods and implementation issues.* Ph.D. thesis, University of Glasgow, UK.

Mudge, S. K., & Patton, R. J. (1988). Enhanced assessment of robustness for an aircraft's sliding mode controller. *Journal of Guidance, Control and Dynamics*, *11*(6), 500–507.

Slotine, J. J. E., & Li, W. (1991). *Applied nonlinear control*, New Jersey, USA: Prentice-Hall International Inc.

Sveen, D. A. (2003). *Robust and adaptive tracking control of surface vessel for synchronization with an ROV: practical implementation on CyberShip II.* Master thesis, Norwegian University of Science and Technology, Trondheim, Norway.

Utkin, V. I. (1972). Equations of the slipping regime in discontinuous systems II. *Automation and Remote Control*, *2*, 211–219.

Zuidweg, J. K. (1970). *Automatic guidance of ships as a control problem*. Ph.D. thesis, Delft University of Technology, The Netherlands.